Advances in Water Resources 54 (2013) 181–190

Contents lists available at SciVerse ScienceDirect

Advances in Water Resources

journal homepage: www.elsevier.com/locate/advwatres

An analytical solution to study substrate-microbial dynamics in soils

Xavier Sanchez-Vila [a,*], Simonetta Rubol [a,b], Albert Carles-Brangari [a], Daniel Fernàndez-Garcia [a]

[a] Hydrogeology Group, Department of Geotechnical Engineering and Geosciences, Universitat Politècnica de Catalunya – BarcelonaTech, Jordi Girona 1-3, 08034 Barcelona, Spain
[b] Dipartimento di Ingegneria Civile ed Ambientale, Università di Trento, Via Mesiano 77, I 38050 Trento, Italy

ARTICLE INFO

Article history:
Received 11 August 2012
Received in revised form 12 February 2013
Accepted 13 February 2013
Available online 21 February 2013

Keywords:
Ecohydrology
Carbon cycle
Soil organic matter
Microbial concentration dynamics

ABSTRACT

We provide an approximate analytical solution for the substrate-microbial dynamics of the organic carbon cycle in natural soils under hydro-climatic variable forcing conditions. The model involves mass balance in two carbon pools: substrate and biomass. The analytical solution is based on a perturbative solution of concentrations, and can properly reproduce the numerical solutions for the full non-linear problem in a system evolving towards a steady state regime governed by the amount of labile carbon supplied to the system. The substrate and the biomass pools exhibit two distinct behaviors depending on whether the amount of carbon supplied is below or above a given threshold. In the latter case, the concentration versus time curves are always monotonic. Contrarily, in the former case the C-pool concentrations present oscillations, allowing the reproduction of non-monotonic small-scale biomass concentration data in a natural soil, observed so far only in short-term experiments in the rhizosphere. Our results illustrate the theoretical dependence of oscillations from soil moisture and temperature and how they may be masked at intermediate scales due to the superposition of solutions with spatially variable parameters.

1. Introduction

Soil biogeochemical cycles, particularly carbon (C), nitrogen (N), and phosphorous (P), are of particular interest in a number of environmental applications involving soil–water interactions [1,7,27]. These include surface–subsurface hydrological inter-exchanges (e.g., [21,26]), water quality evolution during infiltration [10,12], and green-house gas emissions (e.g., [23]). Such biogeochemical cycles are regulated by non-linear dynamic processes acting on multiple spatial and temporal scales [3,4,15,24].

In the present work we concentrate on the carbon cycle. It involves the presence of separate pools corresponding to the different states where organic carbon can be found. It is widely recognized that carbon decomposition is a process driven by bacteria, fungi, archaea and other groups, which can be either enhanced or inhibited by variations in water content and general environmental conditions taking place at different spatial as well as temporal scales [24,28]. Currently, several models (of various complexity) exist to provide the evolution of the C-cycle (and also the N- and P-cycles) in terms of hydro meteorological conditions. The simplest model would involve a single carbon pool. However, as explained in [18], the one C-pool model is not accurate enough to investigate the evolution of biomass concentration due to changes in external climate forcing. For multiple-pool models we can also distinguish between linear and non-linear models. In the former, the decomposition rate is proportional to the substrate concentration; they are oversimplistic and unable to reproduce the observed interactions between microbes and their substrate at short time scales [20]. Different non-linear models have thus been proposed in the literature, where decomposition is governed by some relationship between both the concentrations of substrate and biomass activity [9,16,17,19].

Understanding the dynamics of the interactions atmosphere/biosphere involving for example the water content variations is important to better define processes such as soil quality, the respiration process (gas emissions), and the dynamics of the biomass concentrations. There is a strong non-linear link between the biological processes taking place at the soil (such as biomass decomposition and microbial activity) and a number of environmental factors including soil water content. For example, hydrologic conditions affect many abiotic factors such as soil aeration and nutrient availability so that microbial activity is inhibited at the local scale (e.g., [26]).

The non-linearities already cited may eventually lead to complex evolution of the concentration of carbon at the different pools, involving for example the potential oscillatory behavior of the concentrations measured as a function of time due to a sudden change in the conditions. The presence of oscillations provided in the predator–prey model defined by biomass and their substrate has been reported in some cases, but the physics of the non-linear fluxes

* Corresponding author.
E-mail address: xavier.sanchez-vila@upc.edu (X. Sanchez-Vila).

0309-1708/$ - see front matter © 2013 Elsevier Ltd. All rights reserved.
http://dx.doi.org/10.1016/j.advwatres.2013.02.004

between pools (also known as compartments) have been only partially addressed [24,29,30]. Despite it is widely accepted that oscillations are strongly determined by biomass-substrate interactions, they have only been observed in the rhizosphere at short time scales [30], and it is still questionable whether they may occur on a large time scale or when observations are taken at some intermediate to large spatial scale. According to Manzoni and Porporato [18], in a long term analysis oscillations in C-pool concentrations may be masked by external climate constraints and substrate availability.

In this work we used the non-linear simplified C model of Manzoni and Porporato [18] to illustrate the physics of the oscillatory behavior in carbon-pool concentrations. We started by finding an approximate analytical solution for this model as a function of plant residue addition, soil temperature and soil water content. We then used this solution to derive a closed-form mathematical condition for oscillations in concentrations versus time to occur at a given point in the soil. Next, we analyzed which type of ecosystems are most likely to present oscillations in C-pool concentrations by considering typical litter addition values for different environments and studying the effects of soil moisture, temperature and nitrogen limitation. Finally, we assumed a log-normal distribution for the maximum rate of decomposition and microbial dead, and used this information to investigate under which conditions the upscaling of concentration point value may lead to no observed oscillations at an intermediate scale, illustrating a potential reason why concentration oscillations at a large scale have not yet been reported.

2. Problem statement

2.1. The carbon cycle model

Different operational methods exist to divide the carbon organic matter supplied to a given system into compartments or pools (e.g., [2]). In all of them, the organic carbon supplied to the soil is decomposed into one or more abiotic pools and a biotic one [5], where the latter regulates the fluxes between soil and atmosphere.

In this paper the C-cycle is modelled using two carbon pools following the work of Manzoni and coworkers [20]: the substrate pool, expressed in terms of substrate concentration C_s [M L^{-3}] including the litter and the humus fractions of Soil Organic Matter (SOM-C), and the biomass pool (its concentration denoted by C_b [M L^{-3}]), accounting for the biotic component. A table of all the symbols used throughout the paper, with their corresponding units, is included as Table 1.

The input to the system is provided by addition of plant residue (or alternatively, litter) expressed as mass of carbon per unit of volume and time (ADD^* [M L^{-3} T^{-1}]), while the output is given by microbial respiration, which is expressed as a fraction r of the total decomposition rate (DEC [M L^{-3} T^{-1}]). The decomposition rate is linearly proportional to the product of the two concentrations (substrate and biomass). The exchange between pools is given by equilibrium between the fraction of decomposition that does not result in microbial respiration, and the microbial decay or lysis (BD), as shown in Fig. 1. The system of ordinary differential equations (ODEs) describing the carbon balance for the two-pool system is given as

$$\begin{cases} \frac{dC_s(t)}{dt} = ADD^* - DEC + BD \\ \frac{dC_b(t)}{dt} = (1-r)DEC - BD \end{cases} \quad (1)$$

The microbial decay is most often modeled as a linear function of biomass, $BD = k_d^* C_b$, with k_d^* [T^{-1}] the biomass decay constant, being a characteristic of the actual microbial population. As indicated before, the decomposition rate is linear with respect to

Table 1
List of symbols.

Parameter	Units	Name/description
C_s/C_b	M L^{-3}/M L^{-3}	Substrate/Biomass concentration
C_r	M L^{-3}	Reference concentration
X_s/X_b	−/−	Substrate or SOM/Biomass dimensionless concentration
X_s^{st}/X_b^{st}	−/−	Substrate/Biomass steady-state dimensionless concentration
$X_{s,0}/X_{b,0}$	−/−	Substrate/Biomass initial dimensionless concentration
X_s'/X_b'	−/−	Substrate/Biomass perturbative dimensionless concentration
$\delta_b(=\delta)/\delta_s$	−/−	Substrate/Biomass perturbative initial dimensionless concentration
ADD^*/ADD	M L^{-3} T^{-1}/−	Dimensional/Dimensionless plant residue supplied
ADD_0/ADD_{s-s}	−/−	Initial/Asymptotic amount of plant residue supplied
ΔADD	−/−	Incremental value of plant residue supplied
DEC	M L^{-3} T^{-1}	Total decomposition rate
BD	M L^{-3} T^{-1}	Microbial decay (or lysis)
r		Respiration rate
k_d^*/k_d	T^{-1}/−	Dimensional/Dimensionless biomass decay constant
k_s^*/k_s	L^3 M^{-1} T^{-1}/−	Dimensional/Dimensionless potential decomposition rate
k_r	T^{-1}	Reference reaction rate
φ	–	Coefficient controlling N availability for decomposition
$f_D(s,T)$	–	Reducing factor depending on soil moisture (s) and temperature (T)
s_{fc}	–	Soil moisture at field capacity
$T_{\min}/T_{ref}$	K/K	Minimum/Reference temperature
γ	–	Exponential decay factor regulating the change in ADD with time
ξ	–	Decay constant
t_c	–	Characteristic dimensionless time
ω	–	Angular frequency of the oscillations
a, b, α, β	–	Different parameters defined in the text
Δ	–	Discriminant
P, Q		Auxiliary spatial functions
$\langle\cdot\rangle$		Expected value
σ_i^2/γ_i	–	Variance/Variogram of spatial random function i ($i = s,b$)
λ_1, λ_2		Eigenvalues of the system matrix
C_1, C_2		Integration constants

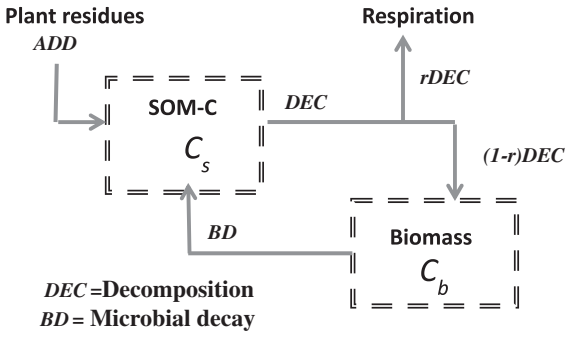

Fig. 1. The organic carbon two-pool system and their corresponding transfer processes to account for the redistribution of SOM-C into a biotic (biomass) and an abiotic (substrate) pools. Plant residual (ADD) and dead microbial mass sustain the carbon pool (C_s), which is decomposed by microbes (C_b) to obtain food and energy, with a fraction (r DEC) lost in respiration.

both concentrations, and therefore it can be modeled as $DEC = \varphi k_s^* f_D(s,T) C_s(t) C_b(t)$. Here φ is a coefficient belonging to the interval [0,1], indicating whether the system is controlled by the availability of nitrogen; thus, φ is equal to one when N is not a limitation for decomposition of organic matter, and becomes smaller than one when the system becomes N-limited (*i.e.* microbes need to use N minerals as the source of nitrogen); k_s^* [L^3 - M^{-1} T^{-1}] is the potential decomposition rate (which depends on the actual substrate being supplied); finally $f_D(s,T)$ is a dimensionless reducing factor depending non-linearly of soil moisture (s) and temperature (T), through $f_D(s,T) = f_1(s) f_2(T)$ as described in Porporato et al. [22]. These functions are themselves modeled as

$$f_1(s) = \begin{cases} s/s_{fc} & if \quad 0 \leqslant s \leqslant s_{fc} \\ s_{fc}/s & if \quad s_{fc} < s \leqslant 1 \end{cases} \tag{2}$$

$$f_2(T) = \begin{cases} 0 & \text{for} \quad T < T_{\min} \\ \frac{(T-T_{\min})^2}{(T_{ref}-T_{\min})^2} & T_{\min} \leqslant T \leqslant T_{ref} \\ 1 & T > T_{ref} \end{cases} \tag{3}$$

where s_{fc} is the soil moisture at field capacity, $T_{\min}$ is a temperature inhibiting microbial respiration, and T_{ref} is a reference temperature [13]. We refer to [18] for a thorough explanation of the immobilization and mineralization conditions and of the environmental functions, as well as some indications on the range of validity of the parameters involved in Eqs. (2) and (3).

In order to measure the importance of different rates, we use a dimensionless version of the model by using a reference concentration C_r [M L^{-3}], and a reference reaction rate k_r [T^{-1}], so that the dimensionless time t_r and concentrations X_i ($i = s,b$) can be defined as follows:

$$\begin{aligned} t_r &= t k_r \\ X_i &= C_i / C_r \quad i = s,b \end{aligned} \tag{4}$$

By inserting expression (4) into Eq. (1), the system of equations governing the problem in terms of dimensionless concentrations is rewritten. The subindex r in the dimensionless time (4) is dropped here and in the remaining of the text for simplicity.

$$\begin{cases} \frac{dX_s(t)}{dt} = ADD - \varphi k_s f_D X_s(t) X_b(t) + k_d X_b(t) \\ \frac{dX_b(t)}{dt} = (1-r)\varphi k_s f_D X_s(t) X_b(t) - k_d X_b(t) \end{cases} \tag{5}$$

where the following dimensionless parameters have been included

$$ADD = \frac{ADD^*}{k_r C_r}; \quad k_s = \frac{k_s^* C_r}{k_r}; \quad k_d = \frac{k_d^*}{k_r} \tag{6}$$

It should be noted that in a general problem k_s, k_r could be time dependent as a consequence of changes in the biochemical system such as aging. Such changes take place at large time scales, and so it is considered here that in the characteristic time where (5) holds, temporal variations in such parameters are negligible.

2.2. Steady state solution

By imposing steady state conditions in Eq. (5), the following expression for the steady state concentrations can be derived

$$X_s^{st}(s,T) = \frac{k_d}{(1-r) k_s \varphi f_D(s,T)} \quad X_b^{st} = \frac{ADD_{s-s}(1-r)}{k_d r} \tag{7}$$

ADD_{s-s} corresponds to the asymptotic amount of plant residue supplied; it is assumed constant since otherwise the solution would not reach an steady-state value. The solution could also be used for variable ADD if the time variations take place at a scale much larger than the time needed by the system to reach steady-state.

For steady state conditions, the substrate pool concentration depends on soil moisture and temperature as an inverse dependency upon $f_D(s,T)$. It also depends on whether N becomes a limiting factor for organic matter decomposition, so that the smaller the φ value, the larger the asymptotic concentrations remaining at the substrate pool. The biomass pool, instead, depends linearly on the external input of plant residue supplied, and it is mostly controlled by the respiration rate.

2.3. Semi-analytical solution for an exponential ADD input

By using a fist-order perturbation approach, it is possible to derive an (approximate) fully analytical solution for a number of problems with varying boundary and initial conditions. First, a system in dynamic equilibrium is considered, indicating that the plant residue or litter input, ADD_0, is equilibrated with the losses due to respiration; the dimensionless concentrations in the two carbon pools are then given by (7). Then a variation in the supply takes place following an exponential function, asymptotically reaching a value ADD_{s-s}. The solution is derived in Appendix A, and reported here as Eqs. (8) and (9). It indicates that the evolution of the substrate and biomass pool concentrations are both given as combinations of an exponential decay term (with a decay constant $\xi = -a/2$, equivalent to a characteristic dimensionless time $t_c = 2/|a|$), multiplied by sinusoidal functions with an angular frequency of the oscillations $\omega = \frac{1}{2}\sqrt{|\Delta|}$,

$$\begin{aligned} X_s(t) = X_s^{st} &+ \alpha \exp(-\gamma t) \\ &+ \frac{2b}{\sqrt{|\Delta|}} \left(\delta - \beta - \frac{\alpha a}{2b}\right) \exp\left(\frac{at}{2}\right) \sin\left(\frac{1}{2}\sqrt{|\Delta|} t\right) \\ &- \alpha \exp\left(\frac{at}{2}\right) \cos\left(\frac{1}{2}\sqrt{|\Delta|} t\right) \end{aligned} \tag{8}$$

$$\begin{aligned} X_b(t) = X_{b,1}^{st} + \beta \exp(-\gamma t) + \frac{-2ab\delta + 2ab\beta + \alpha a^2 + \alpha|\Delta|}{2b\sqrt{|\Delta|}} \\ \times \exp\left(\frac{at}{2}\right) \sin\left(\frac{1}{2}\sqrt{|\Delta|} t\right) + (\delta - \beta) \\ \times \exp\left(\frac{at}{2}\right) \cos\left(\frac{1}{2}\sqrt{|\Delta|} t\right) \end{aligned} \tag{9}$$

where γ is the exponential decay factor regulating the change in ADD with time, δ is the difference between the (dimensionless) biomass concentration at steady state (Eq. (7)) and the initial one, a, b, α, β are coefficients given respectively by $a = -\frac{ADD_{s-s} f_D k_s \varphi (1-r)}{k_d r}$; $b = -\frac{k_d r}{(1-r)}$; $\alpha = \frac{\gamma \Delta ADD}{\gamma^2 + a\gamma - ab(1-r)}$, $\beta = -\frac{(1-r)a\Delta ADD}{\gamma^2 + a\gamma - ab(1-r)}$, and $\Delta = a^2 - 4ab(1-r)$ is the discriminant of the characteristic polynomial of the system of equations. The solution presented in Eqs. (8) and (9) is only valid for the case $\Delta < 0$. A more general solution, valid also for positive Δ values is also reported in Appendix A.

As stated before, other solutions could be obtained by varying either the boundary or the initial conditions. Appendix B reports the solution corresponding to a problem where no changes in the input take place, but where the system is initially not in equilibrium.

3. Discussion

The advantage of an analytical approximation providing an explicit solution for the SOM-C pool concentrations with respect to a fully numerical one is the possibility of analyzing directly the impact of the different parameters in the solution. Furthermore, it is possible to fully account for the combination of parameters resulting in an oscillatory (non-monotonic) solution, and in

Table 2
Parameters used in the different plots used as examples in this paper (unless different values are reported in the text).

Parameter	k_d [d^{-1}]	k_s [d^{-1}]	φ [-]	s_{fc} [−]	$T[K] = T_{ref}$
Value	$8.5\ 10^{-3}$	$6.5\ 10^{-5}$	1	0.3	293.15

such a case, to understand the interplay between the exponential decreasing part and the sinusoidal part in Eqs. (8) and (9). In the following subsections several points are discussed: (i) a close-form inequality to warrant the presence of oscillations of the solution at the local scale; (ii) the performance of the analytical solution; (iii) the impact of different environmental factors in the solution; and (iv) the upscaling of the analytical solution when parameters are assumed spatially and temporally heterogeneous.

3.1. Validity of the approximate solution

The closed form analytical solutions presented throughout this paper are based on a combination of a perturbation expansion followed by a closure (elimination of high order terms). Thus, it is necessary to investigate the range of validity of the approximate solution. This depends on the error introduced in the solution by neglecting the product of perturbations of the two dimensionless concentrations. Both at time zero and for infinite times the perturbation X_s' is zero, and so the approximate solution is exact. On the other hand, the approximation deteriorates at short (but non-zero) times.

The solution provided by Eqs. (8) and (9) is then tested by comparing it to that obtained from a high-resolution numerical code designed to solve the full system of partial differential equations (5) with no approximations. The code uses the MATLAB's standard solver for ODEs (ODE45) with an explicit method implementing a Runge–Kutta algorithm, with a variable time step for efficient computation. This numerical solution can be considered as exact for all practical purposes. The parameters used for the comparison are considered constant and known, and are extracted from a savanna region characterized by [24], and summarized in Table 2; furthermore $\gamma \to \infty$, equivalent to a sudden change in the *ADD* value. Two different values of ΔADD are used in the simulations, ranging from a small jump to quite a large one (relative to the initial value ADD_0).

The results of the comparison are presented as Fig. 2. Three significant features must be highlighted: First, the analytical solution is capable of properly reproducing the presence of oscillations in the concentration versus time function, in particular in terms of frequency and phase of oscillations; this is remarkably important because it renders the criterion to distinguish between oscillatory and monotonic behavior presented in the next section to be robust and highly insensitive to the value of ΔADD. Second, both numerical and analytical solutions seem to approach steady-state conditions at a similar rate; this means that the characteristic time to reach steady state given by the analytical solution is a good estimate of its true value regardless the degree of the ΔADD jump. Third, the exact amplitude of the oscillations is not perfectly reproduced, and the match deteriorates when large initial perturbations are imposed to the system.

3.2. The condition for oscillations to occur

The critical condition for an oscillatory behavior to occur can be obtained in closed form by imposing that the discriminant is negative (i.e. $\Delta < 0$, implying that the eigenvalues of the characteristic matrix are complex numbers with a non-zero imaginary part). For a given ecosystem, this condition can be used to determine the range of the external plant residue input (ADD^*) that will promote oscillations in the temporal evolution of concentrations in the SOM-C system. This condition can be written (in dimensional quantities) as

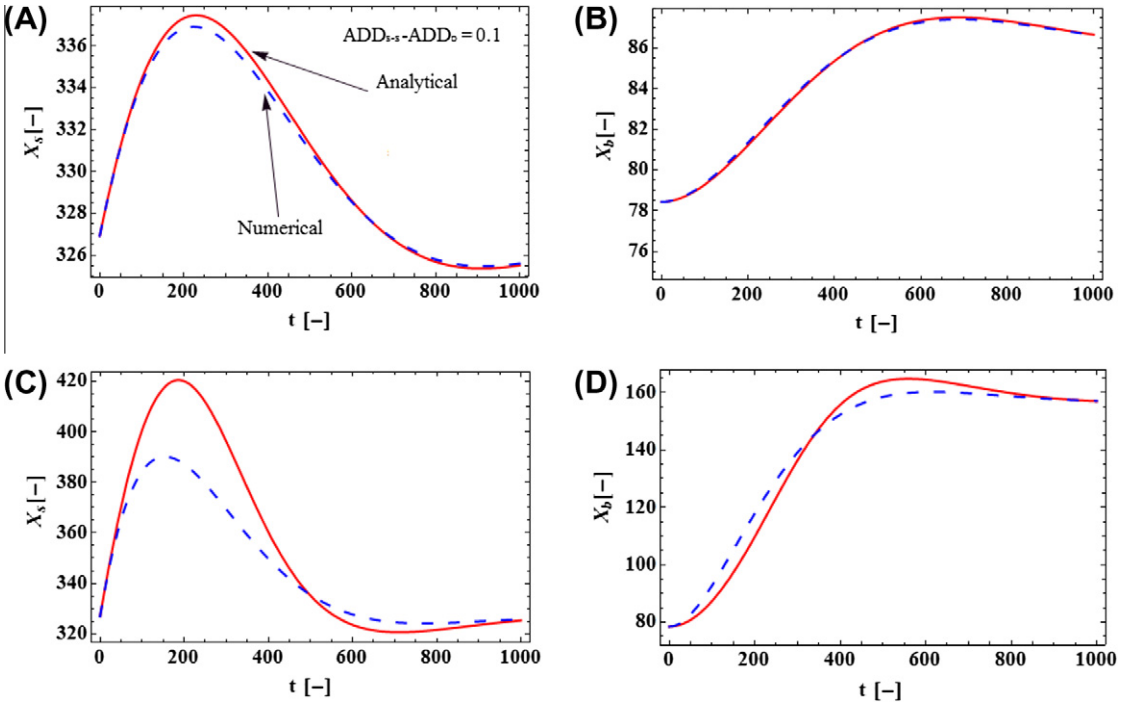

Fig. 2. Comparison of the analytical (approximation) solution and the exact one (obtained by a numerical approach). The perturbation approach implies that for small jumps (with respect to the initial value) in *ADD* values (top), the analytical solution provides a very good match to the true solution. The agreement deteriorates for large *ADD* jumps (bottom), but the main features are captured.

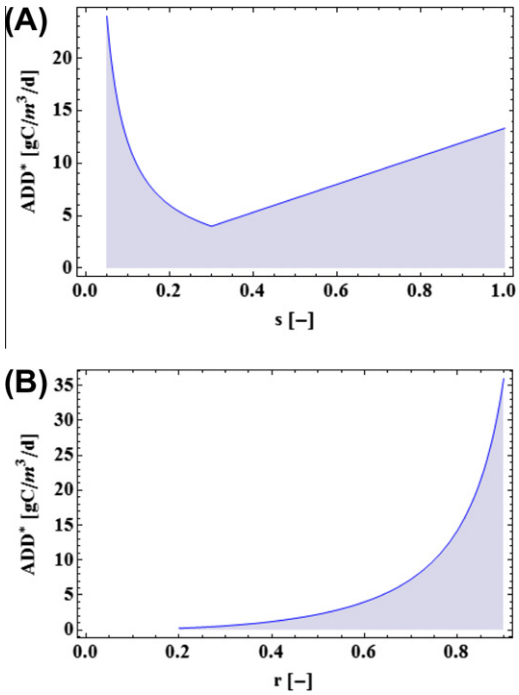

Fig. 3. (A) Mapping in the ADD^* vs. soil moisture space showing the combination of values where oscillations are likely to occur (shaded); (B) similar plot for the impact of the respiration rate (r), for a fixed soil moisture $s = s_{fc}$ value. Additional parameters values presented in Table 2. If the combination of parameters can be displayed in a non-shaded area, a monotonic variation in the concentrations is expected.

$$0 < ADD^* < \frac{4k_d^{*2}r^2}{\varphi f_D k_s^*(1-r)} \tag{10}$$

For values of ADD^* outside the range of Eq. (10), the SOM-C pool concentrations experience a monotonic, non-oscillatory, behavior from its initial value to the asymptotically reached steady-state one. This is expected to occur in systems where the plant residue input is rich in labile organic carbon. However, even for plant residue inputs belonging to the range defined in (10), oscillations in C-concentrations with time may not be "visible" given that the exponential decreasing term may overcome the sinusoidal term in (8) and (9), so that the small errors in the measurements may mask the actual oscillations.

Using again the parameters from Table 2, Fig. 3A presents a map in the ADD^* vs. soil moisture (s) space showing the combination of values (shaded zone) where oscillations would occur (i.e., $\Delta < 0$), and that where a monotonic behavior is expected ($\Delta > 0$). The two zones are separated by a solid line expressing the change in behavior, displaying a minimum at soil moisture $s = s_{fc}$. Since according to [25] for natural systems the value of the critical plant residue input can be estimated to be in the range of 0–16 gC/m^3/d, it is to be expected that in most cases oscillations at the local scale should be the rule rather than the exception.

Fig. 3B additionally displays the impact of the variations in the respiration rate (r) upon the behavioral solution (oscillating vs. non-oscillating). For small r values the system becomes stable for almost all combinations of the remaining parameters; it implies that no carbon is removed from the system (*i.e.*, high microbial uptake and low respiration) and it is mostly a redistribution problem with a comparative negligible substrate pool, producing an almost linear accumulation of carbon in the biomass; such an unphysical result could be avoided by incorporating additional decomposition terms in (5). Another extreme case is to consider a very large value

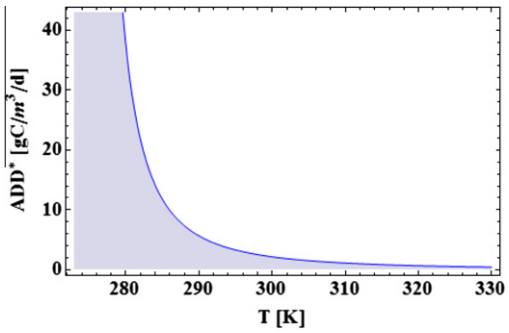

Fig. 4. Mapping in the ADD^* vs. temperature space showing the combination of values where oscillations would occur (shaded area); we assume T_{min} = 273.15 K, and a T_{ref} value of 293.15 K. Additional parameters values are displayed in Table 2.

of r, indicating that no decomposition ends up in increasing the biomass pool concentration (no carbon is metabolized), so that this pool is non-existing (thus becoming a degenerative solution). This aspect could be relevant in some real problems, although the study of factors regulating respiration rates is still lacking in the literature.

Fig. 4 includes the impact of temperature in the oscillatory behavior of the solution. When T is close to T_{min} the system cannot reach monotonically a steady solution for any combination of parameters. Apparently this result contradicts the observed system dynamics in chronically cold systems, like tundra, where decomposition is consistently slow and inherently stable (e.g., [8,11]) associated to the fact that cold temperatures do not give favorable conditions for organic matter decomposition. The actual explanation is given by the fact that Δ, and thus ω is very small, resulting in a very large period of the oscillations that could be wrongly mistaken with a monotonic behavior.

Figs. 3 and 4 are representative of a system with low substrate C:N ratio (i.e., $\varphi = 1$). However, in natural systems N may be the limiting factor (e.g., [14]). Under N-limiting conditions, microbes need to use the mineral pools as a source of nitrogen and if this source is not enough to match the C:N ratio of the microbes, decomposition must be reduced to meet the actual availability of N. The model here presented does not try to mimic explicitly the N-dynamics, and so all dependence of nitrogen on the C-cycle is accounted by means of the φ factor. The net effect of N being totally or partially a limiting factor in the C-cycle ($\varphi < 1$) is inversely seen in the threshold value in Eq. (10). The area where we are prone to find an oscillatory solution increases with decreasing φ values (see Fig. 5). Notice that $\varphi = 0$ would be a degenerative (unphysical) solution.

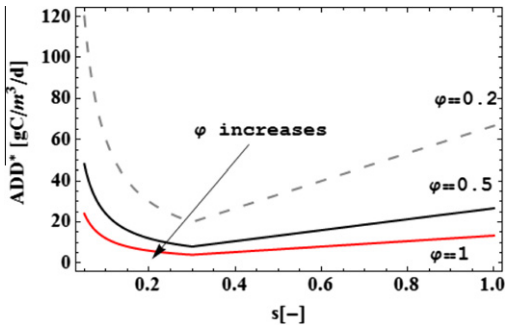

Fig. 5. Mapping in the ADD^* vs. soil moisture space showing the combination of values where $\Delta = 0$ for different φ values corresponding for different N-limited conditions. The areas where oscillations occur are always located below the lines drawn. Additional parameters values are displayed in Table 2.

The analysis presented so far indicates that oscillations in the concentration evolution with time may be enhanced when the environmental conditions are far from standard reference conditions and are associated to conditions which are adverse to microbial activity. In summary, it thus should be expected that oscillations prevail in systems that are either (1) very dry or very close to saturation conditions, (2) for large respiration rates, (3) when the soil temperature is very low, or (4) when the system is N-limited.

3.3. Competition between ξ and γ

The analytical solution presented has two characteristic times associated to the parameters characterizing the exponentials, i.e., γ and ξ. The former characterizes the shape of the organic matter supply function, while the latter combines the different parameters dealing with the decomposition of organic matter into the different pools and characterizes the respond of the system. Depending on the value of the parameters, a very distinct behavior of the solution can be observed. For a fixed ξ value, a value of $\gamma \to \infty$ implies a sudden (instantaneous) change in the supply of organic carbon. In such a case, $\alpha = \beta = 0; \quad C_1 = -C_2 = \delta/\sqrt{|\Delta|}$, and the solution for the concentration values as a function of time (assuming $\Delta < 0$) simplifies to

$$X_s(t) = X_s^{st} + \frac{2b\delta}{\sqrt{|\Delta|}} \exp\left(\frac{at}{2}\right) \sin\left(\frac{1}{2}\sqrt{|\Delta|}t\right) \tag{11}$$

$$X_b(t) = X_{b,1}^{st} - \frac{a\delta}{\sqrt{|\Delta|}} \exp\left(\frac{at}{2}\right) \sin\left(\frac{1}{2}\sqrt{|\Delta|}t\right) + \delta \exp\left(\frac{at}{2}\right) \cos\left(\frac{1}{2}\sqrt{|\Delta|}t\right) \tag{12}$$

that is, the system responds by trying to reach steady state at some characteristic time $t_c = 2/|a|$. The other limiting case would be that of $\gamma \to 0$. In such a case the system degenerates to the following solution

$$X_s(t) = X_s^{st}, \quad X_b(t) = X_{b,1}^{st} + \frac{\Delta ADD}{b} \exp(-\gamma t) \tag{13}$$

indicating that the solution displays a constant concentration for the substrate pool and a monotonic behavior for the biomass pool, fully driven by the external function controlling plant residue input. No oscillations are observed in this case regardless of the combination of parameters.

An example of this behavior is shown in Fig. 6. Fig. 6B shows the evolution of the biomass pool (normalized) concentration versus time for different values of γ. For better identification Fig. 6A shows the function of *ADD* supply for the different γ values. The remaining parameters are those in Table 2. The figure shows the transition in behavior related to the analyzed range of γ values.

3.4. Competition between exponential decay and sinusoidal oscillations

From (8) and (9), the evolution in time of the substrate and biomass pool concentrations is given by a combination of an exponential and a sinusoidal function. The former is controlled by the value of ξ (assuming a large γ) and the latter by that of ω. Assuming that all other parameters are constant, oscillations are more visible when k_d is large, since it results in low values of ξ, with little impact on ω. The opposite occurs for large k_s values, resulting in the exponential being the dominant behavior so that oscillations are hardly visible and could be obscured in experimental data even at point scale. An example of the two types of behavior can be seen in Fig. 7. On the top row an example of a low oscillating solution (large relative k_s value) is presented; the bottom row shows an example corresponding to a large k_d value.

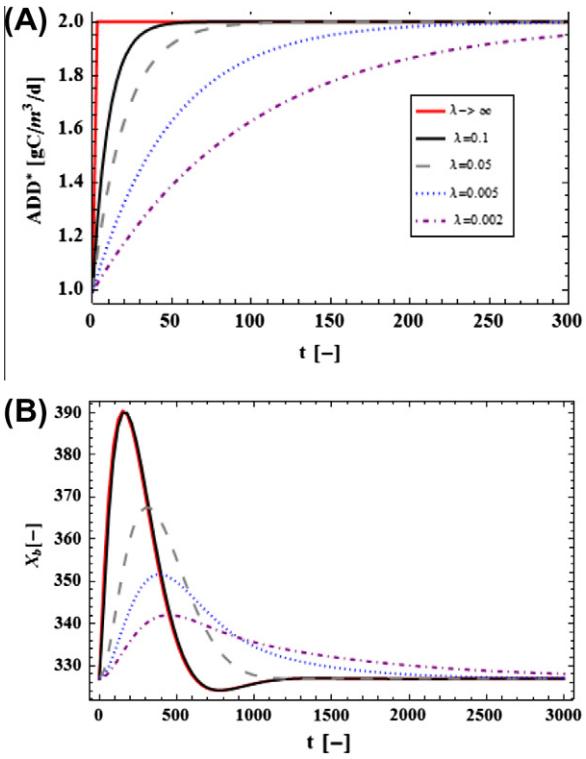

Fig. 6. (A) shape of the ADD^* supply function for different γ values, and (B) the corresponding evolution of the biomass pool (normalized) concentration versus time. The remaining parameters are those in Table 2. The largest the γ value (indicating larger derivative at very small times), the larger the amplitude of the oscillations, and the earlier the peak of the first oscillation occurs.

3.5. Local-scale solutions

The solution procedure can be extended to generate a suite of analytical explicit solutions with different initial conditions, allowing a fast calibration of the different parameters involved in the (two-pool) model under specific conditions. We compare here an analytical solution with data coming from a real site. The test site and the experiment is described in Zelenev et al. [29], and was already analyzed by Manzoni and Porporato [18] transforming the raw data into temporal evolution of concentration. The raw data correspond to biomass concentration measures at the plant-root scale (thus can be considered point measurements), and are presented in Fig. 8. Albeit some noise is present, the authors described the data as displaying an oscillatory behavior. Oscillations show a wavelength close to 250 h and a slow decay in peak concentration with time (about 5% reduction after two cycles).

Based on the description of the experimental setup provided by [29] and [18], the model presented in Appendix B that assumes a constant *ADD* input in a system that is initially not in equilibrium was fitted. From the experiment description it was considered $\varphi = f_D = 1$, and $\delta_B = 0$. The respiration rate was set at a fixed value of $r = 0.6$. A sensitivity analysis (not shown) indicates that the solution is highly sensitive to k_s^* and δ_s, while k_d^* can span a wide range of values without affecting the final solution. Thus, $k_d^* = 0.9d^{-1}$ was fixed (similar to the value reported in [18]). The values of k_s^*, δ_s were calibrated manually until the L2 distance between the experimental data and the analytical solution presented in (B.6) was minimized. It should be noted that no data

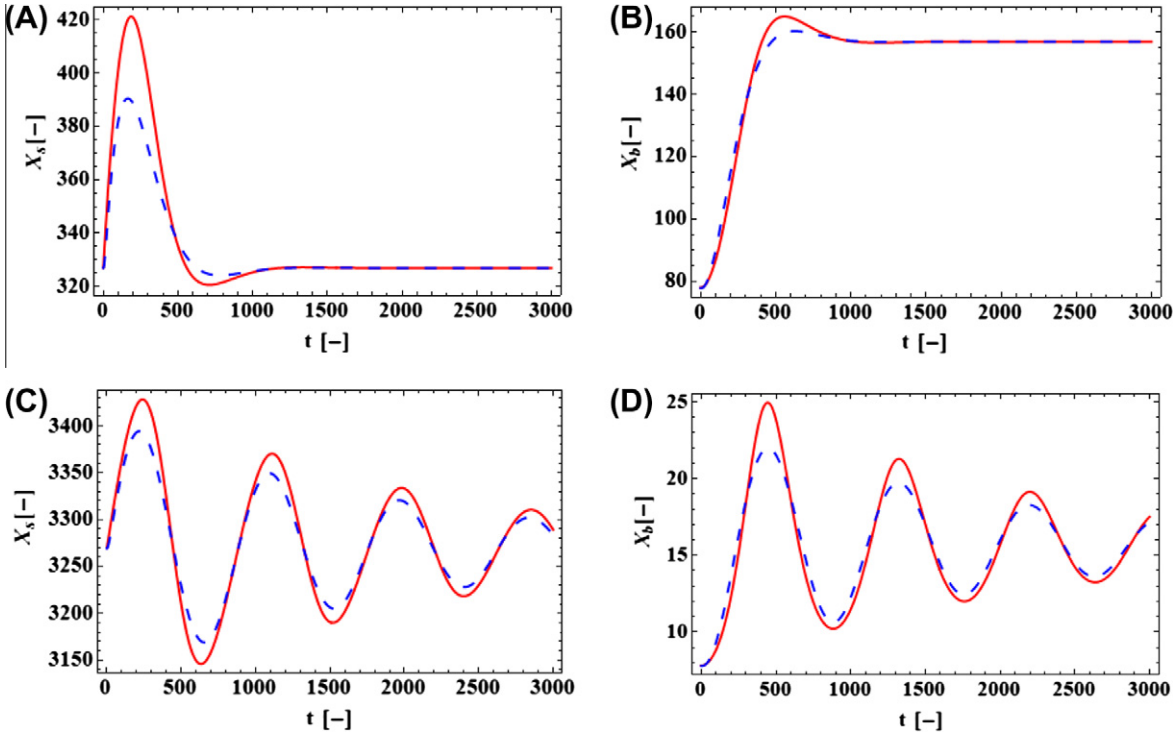

Fig. 7. Performance of the analytical solution for the evaluation of dimensionless concentrations of microbial (X_b) and substrate (X_s) pools as a function of time. Assuming a sudden jump in plant residue input ΔADD = 1 gC/m^3/d with k_d^* = 0.0085 d^{-1} (top row) and 0.085 d^{-1} (bottom). Continuous lines refer to the numerical solution, while dotted lines are those obtained by direct substitution of the parameters in Eqs. (8) and (9). The parameter values used in this comparison are: $\varphi = 1$; k_s^* = 6.5 10^{-5} d^{-1}; ADD_0 = 1 gC/m^3/d; r = 0.6; $s_{fc} = 0.3$. Notice all figures display a different vertical legend to emphasize the qualitative behavior.

was available in the experiment regarding the evolution of X_s with time.

3.6. Spatial variations of concentrations and large-scale solution

The solutions presented so far can be considered local, indicating that they are valid at a point support volume and cannot be directly generalized for larger scales. The steady-state solution is considered first. At each individual point in the soil surface the values for all the parameters r, k_d, k_s, f_D are assumed. All these parameters are spatially variable, so that the steady-state concentrations can be rewritten as

$$X_s^{st}(\mathbf{x}) = P(\mathbf{x}), \quad X_b^{st}(\mathbf{x}) = ADD(\mathbf{x}) \cdot Q(\mathbf{x}) \tag{14}$$

where P, Q are different combination of parameters, derivable from the analogy between Eqs. (14) and (7), and that now are considered spatially random functions. The input plant residue may also be spatially variable. Assuming ADD is a random variable uncorrelated to the different soil parameters, the mean, variance and variogram (assuming the three functions ADD, P, Q are statistically stationary) are written as

$$\langle X_s^{st} \rangle = \langle P \rangle, \quad \langle X_b^{st} \rangle = \langle ADD \rangle \langle Q \rangle \tag{15}$$

$$\sigma^2_{X_s} = \sigma^2_M, \quad \sigma^2_{X_b} = \sigma^2_{ADD}\sigma^2_N + \langle ADD \rangle^2 \sigma^2_N + \langle N \rangle^2 \sigma^2_{ADD} \tag{16}$$

$$\begin{aligned} \gamma_{X_s} &= \gamma_P, \gamma_{X_b} \\ &= \gamma_Q(\sigma^2_{ADD} + \langle ADD \rangle^2) + \gamma_{ADD}\left(\sigma^2_Q + \langle Q \rangle^2\right) - \gamma_Q \gamma_{ADD} \end{aligned} \tag{17}$$

Since both k_d, k_s can be seen as multiplicative processes (similar, for example, to grain surface areas distribution), and thus amenable to be hypothesized to follow a lognormal (LN) distribution. Evidences in the literature indicate that degradation rates might actually be modeled with a LN distribution (e.g. [6]), consistent with our hypothesis. As a direct consequence P, Q are also lognormal. Contrarily, reports about the spatial distribution of ADD are not available in the literature.

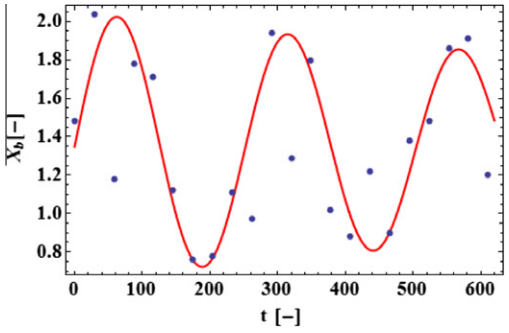

Fig. 8. Data (points) of biomass concentration evolution with time presented in [18] modified from the original data reported by [29]. Best fitting obtained with equation (B.6) with k_s^* = 8.5 10^{-4} d^{-1}; k_d^* = 0.9 d^{-1}. Additional parameter values are presented in the text body. Best fit is obtained by manually minimizing the L2 norm between analytical solution and data points.

From equation (17) the variogram of X_b is expressed as a combination of γ_Q, γ_{ADD}. Thus, the integral scale of X_b is governed by the smallest of the two integral scales of ADD, Q. An upscaling process is now considered. It is assumed that (A.7) is the solution at the point scale, and further that the study area is large compared to the integral scales of the random functions. Then, a moderately large number (over 100) of sampling points are drawn randomly from this large monitored area. On the average this is equivalent to drawing 100 independent identically distributed values of the random variable.

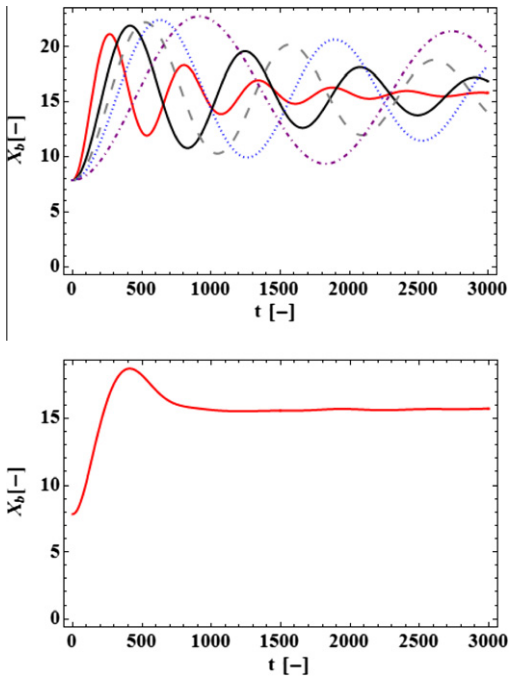

Fig. 9. Example of spatial upscaling for biomass concentration; five selected curves assumed valid at the local scale (top) and the corresponding average (bottom). While individual curves might display oscillations for very large times, such oscillations are cancelled out in the average curve. Each curve has been drawn using constant parameters (defined in the text) except k_s^* which is considered random and drawn from a lognormal distribution LN(−9.64, 1.0) [d^{-1}].

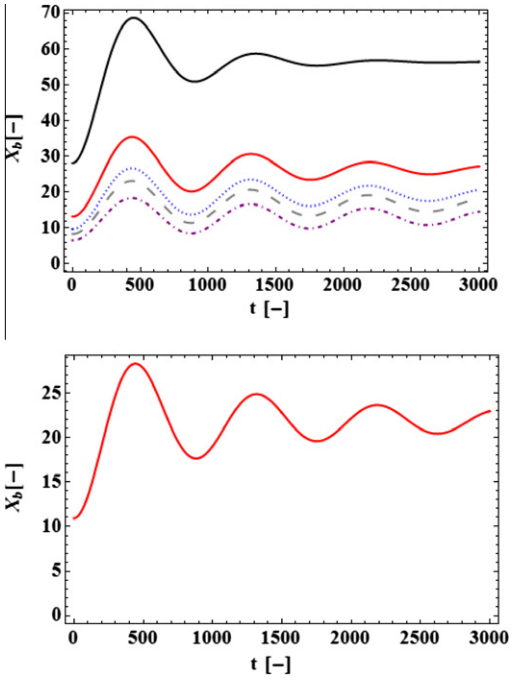

Fig. 10. Example of spatial upscaling for biomass concentration; five selected local scale curves (top) and the corresponding average (bottom). Each curve has been drawn using constant parameters (defined in the text) except k_d^* = LN(−2.47, 1.0) [d^{-1}].

Two cases are considered, varying just one parameter in each one, with the remaining parameters set fixed. In the first one the parameter varying is k_s^*, with each individual realization drawn from a lognormal distribution $k_s^* = \mathrm{LN}(-9.64, 1.0)$ [d^{-1}]. The remaining (fixed) parameters are: $\varphi = 1$; $f_D = 1$; $r = 0.6$; $s_{fc} = 0.3$; $\gamma \to \infty$; $ADD_0 = 1$ gC/m^3/d; $ADD_{s-s} = 2$ gC/m^3/d; and $k_d^* = 0.085 d^{-1}$. Fig. 9 displays 5 (out of the 100) selected curves showing how each individual realization of the biomass concentration function may display an oscillatory behavior extending for large times. On the contrary, the average value shows a very different shape, where oscillations are mitigated. This indicates that in general an average value for k_s^* would not be capable to reproduce the average behavior. The reason is that the average solution involves the sum of sinusoidal curves of different (and random) wavelengths. This is known to produce solutions where sinusoidal effects are cancelled out.

In the second example the random variable is k_d^*, also considered lognormal and $k_d^* = \mathrm{LN}(-2.47, 1.0)$ [d^{-1}]. We further fix $k_s^* = 6.510^{-5}\ d^{-1}$, while the remaining parameters are equal to those of the previous example. The behavior of the solution is quite different, since now the individual realizations are relatively similar between them. The upscaled curve then resembles the shape of the individual curves (Fig. 10).

As a consequence of these two examples, it can be concluded that in some cases it would be easier to observe oscillations in biomass pool concentrations at the small scale, but it would be much more difficult to visualize or measure such oscillations when measurements are taken at some large scale.

4. Conclusions

This work provides a mathematical linearized solution for the evolution of substrate and microbial pool concentrations related to the presence of plant residue or litter input. The biogeochemical model involves decomposition rate from substrate to biomass, biomass decay and an output from the system due to respiration. A condition for the occurrence of oscillations in the pools concentrations as a function of time is provided. It is shown that the occurrence of fluctuations is linked to environmental conditions and changes in input conditions.

The analytical model allows a detailed study of the sensitivity of the solution to the different parameters. Whenever the conditions for oscillations occur, the concentration curve is a combination of exponential and sinusoidal functions. Whether the solution is controlled by one or the other depends on the combination of parameters. Assuming all the other parameters constant, oscillations are more visible when the biomass decay constant k_d is large compared to the rate of microbial production; the opposite occurs for large potential decomposition rate k_s, resulting in the exponential being the dominant behavior so that oscillations are hardly visible and could be obscured in experimental data even at point scale. Regarding the environmental parameters, oscillations in concentrations are likely to occur when the environmental conditions are associated to adverse conditions for microbial activity, either very dry or else very close to saturation conditions, for large respiration rates, and also when the soil temperature is very low or when the system is N-limited.

The analytical solutions presented in this paper allow fast calibration of the different parameters involved in the two-pool model to reproduce the observations at some local scale. The analytical solution allows direct upscaling, providing explicit solutions for the means, standard deviations and variograms of SOM-C pool concentrations. Depending on the combination of parameters, the upscaling process involving the superposition of sinusoidal functions of different wave length, may result in a fast smoothing of oscillations. The upscaling process can be the reason while despite the environmental conditions most likely result in oscillating solutions, the average concentrations at intermediate to large scales would most likely not display oscillations.

Acknowledgements

The authors acknowledge financial support by the Spanish Ministry of Science and Innovation through the projects Consolider-Ingenio 2010 (CSD2009-00065) and RARA-AVIS (GCL2009-1114). SR acknowledges the support of the Provincia Autonoma di Trento and the European Commission within the 7° Programma Quadro – Azioni Marie Curie Cofund, PAT-Outgoing. XS acknowledges support of Program ICREA Acadèmia.

Appendix A

The system of Eq. (5) can be solved analytically considering a perturbations approach around the steady-state conditions. Such conditions can only be achieved if the plant residue input *ADD* is considered constant after a certain time or else approaching a constant value (denoted as ADD_{s-s}) asymptotically. The substrate carbon pool concentrations can thus be defined as their respective steady values plus a perturbation X_i' ($i = s,b$). We consider an exponential function for the plant residue input from an initial value ADD_0 to a value $ADD_{s-s}(= ADD_0 + \Delta ADD)$, so that

$$ADD(t) = ADD_{s-s} + (ADD_0 - ADD_{s-s})\exp(-\gamma t) \tag{A.1}$$

with $\gamma\,[T^{-1}]$ characterizing the exponential function. The solution in this appendix assumes that the system is in initial equilibrium. We then write the biomass concentration as $X_b^{st} = X_{b,0} + \delta$. The steady value of X_s, does not change from the initial value, $X_s^{st} = X_{s,0}$, but an oscillatory behavior of concentrations is observed in some cases (i.e., whenever condition (10) is satisfied). The perturbation approach starts then by defining

$$\begin{cases} X_s(t) = X_s'(t) + X_s^{st} \\ X_b(t) = X_b'(t) + X_b^{st} \end{cases} \tag{A.2}$$

Now, from (5) and assuming that the product of fluctuations is small with respect to the remaining terms in the expansion, *i.e.* $X_s'(t)\cdot X_b'(t) \approx 0$, and after some algebra we can write the governing system of equations in terms of fluctuations

$$\begin{pmatrix} dX_s'/dt \\ dX_b'/dt \end{pmatrix} = \begin{pmatrix} a & b \\ -(1-r)a & 0 \end{pmatrix}\begin{pmatrix} X_s' \\ X_b' \end{pmatrix} + \begin{pmatrix} -\Delta ADD\exp(-\gamma t) \\ 0 \end{pmatrix} \tag{A.3}$$

with

$$a = -\frac{ADD_{s-s} f_D(s) k_s \varphi (1-r)}{k_d r}; \quad b = -\frac{k_d r}{(1-r)} \tag{A.4}$$

Notice that both a and b are negative values. Assuming that soil moisture is constant and not varying in time, the general solution for the fluctuations components is:

$$\begin{aligned} X_s'(t) &= C_1 b\exp(\lambda_1 t) + C_2 b\exp(\lambda_2 t) + \alpha\exp(-\gamma t) \\ X_b'(t) &= C_1\left(-\tfrac{a}{2} + \tfrac{\sqrt{\Delta}}{2}\right)\exp(\lambda_1 t) + C_2\left(-\tfrac{a}{2} - \tfrac{\sqrt{\Delta}}{2}\right)\exp(\lambda_2 t) + \beta\exp(-\gamma t) \end{aligned} \tag{A.5}$$

where,

$$\begin{aligned} &\lambda_1 = \tfrac{1}{2}(a + \sqrt{\Delta}); \quad \lambda_2 = \tfrac{1}{2}(a - \sqrt{\Delta}); \quad \Delta = a^2 - 4ab(1-r); \\ &\alpha = \tfrac{\gamma\Delta ADD}{\gamma^2 + a\gamma - ab(1-r)}; \quad \beta = -\tfrac{(1-r)a\Delta ADD}{\gamma^2 + a\gamma - ab(1-r)}; \\ &C_1 = \tfrac{1}{\sqrt{\Delta}}\left(\delta - \beta - \tfrac{a}{2b}\left(a + \sqrt{\Delta}\right)\right); \quad C_2 = \tfrac{1}{\sqrt{\Delta}}\left(-\delta + \beta + \tfrac{a}{2b}\left(a - \sqrt{\Delta}\right)\right). \end{aligned} \tag{A.6}$$

The behavior of the solution is mostly controlled by the sign of Δ. A positive Δ implies that both eigenvalues of the system matrix (i.e., λ_1, λ_2) are real and negative, and then concentrations converge exponentially to their final steady-state values. On the contrary $\Delta < 0$ imply complex conjugate eigenvalues, and in such a case concentrations display damped oscillations. In the latter case the pool concentrations can be rewritten as

$$\begin{aligned} X_s(t) &= X_s^{st} + \alpha\exp(-\gamma t) \\ &\quad + \frac{2b}{\sqrt{|\Delta|}}\left(\delta - \beta - \frac{\alpha a}{2b}\right)\exp\left(\frac{at}{2}\right)\sin\left(\frac{1}{2}\sqrt{|\Delta|}t\right) \\ &\quad - \alpha\exp\left(\frac{at}{2}\right)\cos\left(\frac{1}{2}\sqrt{|\Delta|}t\right)X_b(t) \\ &= X_{b,1}^{st} + \beta\exp(-\gamma t) + \frac{-2ab\delta + 2ab\beta + \alpha a^2 + \alpha|\Delta|}{2b\sqrt{|\Delta|}} \\ &\quad \times \exp\left(\frac{at}{2}\right)\sin\left(\frac{1}{2}\sqrt{|\Delta|}t\right) + (\delta - \beta) \\ &\quad \times \exp\left(\frac{at}{2}\right)\cos\left(\frac{1}{2}\sqrt{|\Delta|}t\right) \end{aligned} \tag{A.7}$$

Appendix B

For a system which is initially not in equilibrium in either of the SOM-C pools, an explicit analytical solution can be derived for the evolution of concentrations with time. The system to solve is

$$\begin{pmatrix} dX_s'/dt \\ dX_b'/dt \end{pmatrix} = \begin{pmatrix} a & b \\ -(1-r)a & 0 \end{pmatrix}\begin{pmatrix} X_s' \\ X_b' \end{pmatrix} + \begin{pmatrix} 0 \\ 0 \end{pmatrix} \tag{B.1}$$

subject to

$$X_s'(0) = \delta_S, \quad X_B'(0) = \delta_B \tag{B.2}$$

The solution of the system is:

$$X_s' = \frac{\mathrm{i}\exp\left(\frac{at}{2}\right)\left(\sqrt{-\Delta}\delta_S\cos\left(\frac{1}{2}\sqrt{-\Delta}t\right) + (2b\delta_B + a\delta_S)\sin\left(\frac{1}{2}\sqrt{-\Delta}t\right)\right)}{\sqrt{\Delta}} \tag{B.3}$$

$$X_b' = \frac{\mathrm{i}\exp\left(\frac{at}{2}\right)\left(\sqrt{-\Delta}\delta_B\cos\left(\frac{1}{2}\sqrt{-\Delta}t\right) + (-a\delta_B - 2(1-r)a\delta_S)\sin\left(\frac{1}{2}\sqrt{-\Delta}t\right)\right)}{\sqrt{\Delta}} \tag{B.4}$$

with all parameters defined in (A.6). A particular case of the above solution is given when the initial conditions consists in an increase of the substrate pool. In this case δ_B is zero and a simpler version of the solution exists:

$$X_s' = \frac{\delta_S}{\sqrt{\Delta}}\exp\left(\frac{at}{2}\right)\left(-\sqrt{\Delta}Cosh\left(\frac{1}{2}\sqrt{\Delta}t\right) - aSinh\left(\frac{1}{2}\sqrt{\Delta}t\right)\right) \tag{B.5}$$

$$X_b' = \frac{-2\mathrm{i}(1-r)a\exp\left(\frac{at}{2}\right)\delta_S\sin\left(\frac{1}{2}\sqrt{\Delta}t\right)}{\sqrt{\Delta}} \tag{B.6}$$

References

[1] Braden JB, Brown DG, Dozier J, Gober P, Hughes SM, Maidment DR, et al. Social science in a water observing system. Water Resour Res 2009;45.
[2] Bubier JL, Moore TR. An ecological perspective on methane emissions from northern wetlands. Trends Ecol Evol 1994;9(12):460–4.
[3] Burgin AJ, Yang WH, Hamilton SK, Silver WL. Beyond carbon and nitrogen: how the microbial energy economy couples elemental cycles in diverse ecosystems. Front Ecol Environ 2011;9(1):44–52.
[4] Daly E, Oishi AC, Porporato A, et al. A stochastic model for daily subsurface CO_2 concentration and related soil respiration. Adv Water Resour 2008;31(7):987–94. http://dx.doi.org/10.1016/j.advwatres.2008.04.00.
[5] D'Odorico P, Laio F, Porporato A, Rodriguez-Iturbe I. Hydrologic controls on soil carbon and nitrogen cycles: II a case study. Adv Water Resour 2003;26(1):59–70.
[6] Forney DC, Rothman DH. Common structure in the heterogeneity of plant-matter decay. J R Soc Interface 2012. http://dx.doi.org/10.1098/rsif.2012.0122.

[7] Galloway JN, Townsend AR, Erisman JW, Bekunda M, Cai Z, Freney JR, et al. Transformation of the nitrogen cycle: recent trends, questions, and potential solutions. Science 2008;320(5878):889.
[8] Graglia E, Jonasson S, Michelsen A, Schmidt IK, Havstrom M, Gustavsson L. Effects of environmental perturbations on abundance of subarctic plants after three, seven and ten years of treatments. Ecography 2001;24:5–12.
[9] Groffman PM, Butterbach-Bahl K, Fulweiler RW, Gold AJ, Morse JL, Stander EK, et al. Challenges to incorporating spatially and temporally explicit phenomena (hotspots and hot moments) in denitrification models. Biogeochemistry 2009;93(1):49–77.
[10] Hantush MM. Modeling nitrogen–carbon cycling and oxygen consumption in bottom sediments. Adv Water Resour 2007;30(1):59–79. http://dx.doi.org/10.1016/j.advwatres.2006.02.007.
[11] Heal OW, Flanagan PW, French DD, MacLean SF Jr. Decomposition and accumulation of organic matter in tundra. In: Tundra ecosystems: a comparative analysis. Cambridge University Press; 1981, p. 587–633.
[12] Hillel D. Environmental Soil Physics. San Diego: Academic Press; 1998.
[13] Kätterer T, Reichstein M, Andrén O, Lomander A. Temperature dependence of organic matter decomposition: a critical review using literature data analysed with different models. Biol Fertil Soils 1998;27:258–62.
[14] Kaye JP, Hart SC. Competition for nitrogen between plants and soil microorganisms. Trends Ecol Evol 1997;12:139–43.
[15] Kumagai T, Katul GG, Porporato A, et al. Carbon and water cycling in a Bornean tropical rainforest under current and future climate scenarios. Adv Water Resour 2004;27(12):1135–50. http://dx.doi.org/10.1016/j.advwatres.2004.10.002.
[16] Li C, Frolking S, Frolking TA. A model of nitrous oxide evolution from soil driven by rainfall events: 2 model applications. J Geophys Res 1992;97:9777–83.
[17] Maggi F, Gu C, Riley W, Hornberger G, Venterea R, Xu T, et al. A mechanistic treatment of the dominant soil nitrogen cycling processes: model development, testing, and application. J Geophys Res Biogeosci 2008;113(G2):G02016.
[18] Manzoni S, Porporato A. A theoretical analysis of nonlinearities and feedbacks in soil carbon and nitrogen cycles. Soil Biol Biochem 2007;39(7):1542–56.
[19] Manzoni S, Porporato A. Soil carbon and nitrogen mineralization: theory and models across scales. Soil Biol Biochem 2009;41:1355–79. http://dx.doi.org/10.1016/j.soilbio.2009.02.031.
[20] Manzoni S, Porporato A, D'Odorico P, Laio F, Rodriguez-Iturbe I. Soil nutrient cycles as a nonlinear dynamical system. Nonlinear Processes Geophys 2004;11(5–6):589–98.
[21] Marzadri A, Tonina D, Bellin A. A semianalytical three-dimensional process-based model for hyporheic nitrogen dynamics in gravel bed rivers. Water Resour Res 2011;47(11):W11518.
[22] Porporato A, D'Odorico P, Laio F, Rodriguez-Iturbe I. Hydrologic controls on soil carbon and nitrogen cycles: I modeling scheme. Adv Water Resour 2003;26(1):45–58.
[23] Ridolfi L, D'Odorico P, Porporato A, Rodriguez-Iturbe I. The influence of stochastic soil moisture dynamics on gaseous emissions of NO, N_2O, and N_2. Hydrol Sci J 2003;48(5):781–98.
[24] Rodriguez-Iturbe I, Porporato A. Ecohydrology of Water-Controlled Ecosystems: Soil Moisture and Plant Dynamics. Cambridge University Press; 2004.
[25] Rossiter DG. Digital soil resource inventories: status and prospects. Soil Use Manage 2004;20(3):296–301.
[26] Rubol S, Silver WL, Bellin A. Hydrologic control on redox and nitrogen dynamics in a peatland soil. Sci Total Environ 2012;432:37–46.
[27] Runyan CW, D'Odorico P. Hydrologic controls on phosphorus dynamics: a modeling framework. Adv Water Resour 2012;35:94–109. http://dx.doi.org/10.1016/j.advwatres.2011.10.004.
[28] Schimel JP, Weintraub MN. The implications of exoenzyme activity on microbial carbon and nitrogen limitation in soil: a theoretical model. Soil Biol Biochem 2003;35(4):549–63.
[29] Zelenev V, Van Bruggen A, Semenov A. BACWAVE, a spatial–temporal model for traveling waves of bacterial populations in response to a moving carbon source in soil. Microb Ecol 2000;40(3):260–72.
[30] Zelenev V, Van Bruggen A, Semenov A. Short-term wavelike dynamics of bacterial populations in response to nutrient input from fresh plant residues. Microb Ecol 2005;49(1):83–93.